Calculation of the dielectric function in a local representation

S. Brodersen, D. Lukas, and W. Schattke

Institut für Theoretische Physik und Astrophysik, Christian-Albrechts-Universität zu Kiel, Leibnizstraße 15, D-24098 Kiel, Germany
(Received 19 April 2002; published 15 August 2002)

A formula for the dielectric tensor in real-space coordinates is derived. Expanding this formula in a plane-wave basis yields the well-known Adler-Wiser formula [S.L. Adler, Phys. Rev. **126**, 413 (1962); N. Wiser, Phys. Rev. **129**, 62 (1963)], which is appropriate for bulk systems. For systems with broken symmetry like the semi-infinite crystal this approach is not possible and an alternative can be found in localized functions. Therefore, we investigate the expansion of the dielectric function in a linear combination of atomiclike orbitals basis set and compare the results with the usual plane-wave approach. We found very good agreement for the microscopic dielectric function of diamond and GaAs but deviations in the description of local-field effects.

I. INTRODUCTION

Recent developments in electronic structure calculations show an increasing interest in optical properties. The reasons are manifold. Advances in theoretical understanding as well as computer power make the treatment of more sophisticated approximations to the many body problem feasible. It shows up that inclusion of local-field, self-energy, and excitonic effects[1,2] leads to considerably closer agreement with the experiment in comparison with plain random phase approximation (RPA), which was the standard method for many years. On the other side, experimental techniques that allow more direct access to the dielectric function (DF) such as electron energy loss spectroscopy, ellipsometry, and reflection anisotropy spectroscopy (RAS) have been developed.

But not only for a direct comparison between theory and experiment the DF is of importance. It serves as an input for subsequent calculations like the evaluation of quasiparticle and excitonic effects or photoemission spectra. Most calculations are done within the pseudopotential plane-wave framework because of the nice analytic properties of plane waves. If core orbitals or narrow band systems are considered this is not possible, and the wave functions are expanded (at least partly) in localized functions. Still, in most approaches the DF is expressed in Fourier space which makes it necessary to switch from one basis set to another. For systems with broken symmetry a plane-wave approach is not possible.

Therefore, we investigate the expansion of the DF into localized functions. As has been pointed out by Aryasetiawan and Gunnarson,[3] the DF should be expanded into a "product basis," which leads to very large matrix dimensions. To avoid this unfavorable scaling we use an ordinary linear combination of atomic orbitals (LCAO) basis and compare our results with a usual plane-wave calculation.

Localized-basis functions are well-known for there efficiency in electronic-structure calculations. As has been shown by several authors, see, for example, Refs. 4–6, one can perform state of the art *ab initio* calculations for the electronic structure and optical spectra with the LCAO basis. Of course, the minimal set has to be extended for a proper description of the conduction bands. Still, matrix dimensions are considerably smaller compared with a plane-wave expansion. We have implemented an all-electron full-potential LCAO program, based on density functional theory (DFT) in the local density approximation (LDA). It is described in greater detail in the following section.

In order to calculate the dielectric tensor $\vec{\epsilon}(\boldsymbol{q}, \omega)$ in this LCAO basis we first develop a general formula in real-space coordinates. We then show how to transform to a localized-orbital basis using the random phase approximation to the polarization. The LCAO representation of the inverse DF is easily accessible. Transformation to Fourier space, which has to be done only for $\boldsymbol{G} = \boldsymbol{G}' = \boldsymbol{0}$, yields the macroscopic DF. The basic outline of our derivation is given in Sec III.

As an application of our method, we investigate the optical properties of diamond and GaAs. Because diamond is a first-row element pseudopotential calculations need a vast number of plane waves (energy cutoffs of 42 to 50 Rydberg are necessary[7,8]) whereas we found less than 50 localized orbitals per atom to be sufficient for a converged bandstructure. Results are presented in Secs. IV and V.

II. BAND STRUCTURE METHOD

One of the main problems of any electronic-structure program is the evaluation of matrix elements, especially for the Hamiltonian. In a plane-wave basis the integration is easily done with the help of fast Fourier transformation but one has to rely on the pseudopotential approximation. All-electron methods such as LCAO, the augmented-plane-wave (APW), and linear muffin-tin orbital (LMTO) method often expand charge density and potential into auxiliary functions (spherical harmonics, plane waves, or others) to ease the calculation of the integrals. If the full potential is taken into account, i.e., no muffin-tin or atomic-sphere approximations are used, the convergence properties and the implementation are considerably more complicated. A way to avoid all these problems is the direct evaluation of the integrals in real space, which traces back to Ellis.[9] We adopt this method because of its simplicity and flexibility. As integration points, we choose good lattice points (see, e.g., Ref. 10 and references therein), but other techniques like product Gauss-type rules[11] are also possible. Near nuclei the density of integration points is increased to account for the singular behavior of the potential and the fluctuations of the wavefunction. Basis functions

　　　　　　　　　66 085111-1

$\varphi_{ik}(\boldsymbol{r})$, potential $V(\boldsymbol{r})$, and charge density are tabulated on the integration points $\boldsymbol{r}_p$. Thus, the elements of the overlap matrix $S_{ij}(\boldsymbol{k})$ and Hamilton matrix $H_{ij}(\boldsymbol{k})$ are

$$S_{ij}(\boldsymbol{k}) = \int \varphi_{ik}^*(\boldsymbol{r})\varphi_{jk}(\boldsymbol{r})d^3r \qquad (1)$$

$$\approx \sum_p \omega_p \varphi_{ik}^*(\boldsymbol{r}_p)\varphi_{jk}(\boldsymbol{r}_p), \qquad (2)$$

$$H_{ij}(\boldsymbol{k}) = \int \varphi_{ik}^*(\boldsymbol{r})\left(-\frac{1}{2}\triangle + V(\boldsymbol{r})\right)\varphi_{jk}(\boldsymbol{r})d^3r \qquad (3)$$

$$\approx \sum_p \omega_p \varphi_{ik}^*(\boldsymbol{r}_p)\left(-\frac{1}{2}\triangle + V(\boldsymbol{r}_p)\right)\varphi_{jk}(\boldsymbol{r}_p) \qquad (4)$$

with ω_p being the integration weights. The number of good lattice points varies with the system under consideration. For aluminum, e.g., less than 400 points are needed to get well converged valence-band energies, while for high lying conduction states it takes several thousand points. The precision of this Diophantine-type integration method is not as high as product Gauss-type rules, but one gets already with a few hundred points a good approximation to the final result. Especially at degenerated bands one observes a splitting, which is due to the integration error. With increasing number of good lattice points this effect only slowly vanishes. Nondegenerated bands, instead, converge rather fast. In general, we believe that the error in band energies introduced by the numerical integration scheme is of the order of 0.1 eV. For the DF this is surely smaller than errors coming from other sources, like the local density approximation itself or $\boldsymbol{k}$-point sampling.

The choice of basis functions is another important question. Because of the numerical integration we are not restricted to a special kind and tried numerical atomiclike orbitals as well as plane waves and mixed basis sets. To get rid of deep lying core states the basis can be orthogonalized to Bloch sums of atomic core orbitals. We are interested in optical properties. Therefore, a proper description of conduction bands is needed. By comparison of LCAO and mixed-basis calculations it shows up that plane waves are not necessary. The quality of the LCAO basis can be improved in two ways: first, increasing the angular momentum, and, secondly, taking more orbitals for a given angular momentum channel. For open structures, additional functions can be located in the interstitial thereby reducing the angular momentum expansion. Thus, basis-set convergence is achieved in a controlled manner with a modest number of basis functions per atom.

The radial functions $R_{At,nl}(r)$ for a given angular momentum l are calculated by solving the Schrödinger equation for the potential

$$V(r) = V_C(r) + V_{xc}[\varrho(r)] - \frac{Z}{r} + V_{conf}(r) + \frac{l(l+1)}{2r^2}. \qquad (5)$$

Z denotes the atomic number, V_{xc} the exchange-correlation potential, and V_C the Coulomb potential. The latter contain the radial-density $\varrho(r)$.

$$V_{conf}(r) = \left(\frac{r}{r_0}\right)^4 \qquad (6)$$

is a confinement term[12] which damps the orbitals rapidly to zero for $r>r_0$. This additional potential leaves the physical properties of the orbitals, like the number of nodes and the behavior for $r\to 0$ and $r\to\infty$, unchanged. The Hamiltonian of the crystal is not affected by the artificial potential V_{conf}. The parameter r_0, which depends on the angular momentum l, is chosen to be

$$r_0 = \left(\frac{x_l R_{nn}}{2}\right)^{3/2}, \qquad (7)$$

with R_{nn} being the distance to the nearest neighbor. x_l is roughly one. The exact value is not important as long as there are enough basis functions. We found x_0 in the range 1 to 1.2 and $x_l=1$ for $l>0$ to be a good choice for a wide variety of substances. The off-site orbitals are determined in the same way but V_C, V_{xc}, and Z are all zero.

From the atomic orbitals $u_{At,nlm}(\boldsymbol{r}) = R_{At,nl}(r)Y_{lm}(\hat{\boldsymbol{r}})$ (Y_{lm} denote spherical harmonics) Bloch sums are formed and tabulated on the integration points for each Bloch vector $\boldsymbol{k}$:

$$\varphi_{ik}(\boldsymbol{r}) = \frac{1}{\sqrt{N}}\sum_{\boldsymbol{R}} e^{i\boldsymbol{k}\cdot\boldsymbol{R}} u_i(\boldsymbol{r}-\boldsymbol{R}-\boldsymbol{s}_i). \qquad (8)$$

The superindex i stands for position $\boldsymbol{s}_i$ and kind At of the atom and the quantum numbers nlm. The normalization constant N gives the number of unit cells in the crystal.

The Kohn-Sham equations are iterated to self-consistency with an acceleration scheme due to Anderson,[13] which is mathematically equivalent to Broyden's method.[14] Integration over the Brillouin zone is done with special points for insulators or good lattice points for metals when more $\boldsymbol{k}$ points are required. The exchange-correlation potential is due to Ceperley and Alder[15] as parametrized by Perdew and Zunger.[16]

III. DIELECTRIC FUNCTION

A test charge ϱ_i placed into a crystal will lead to a potential V_i and an electric induction $\boldsymbol{D}$. In Fourier space, with each momentum vector composed of a reciprocal lattice vector $\boldsymbol{G}$ and a vector $\boldsymbol{q}$ confined to the 1 Brillouin zone, the relation is

$$\boldsymbol{D}(\boldsymbol{G}+\boldsymbol{q},\omega) = -i(\boldsymbol{G}+\boldsymbol{q})V_i(\boldsymbol{G}+\boldsymbol{q},\omega). \qquad (9)$$

A similar equation holds for the electric field $\boldsymbol{E}$ and the total potential $V=V_s+V_i$, V_s being the potential of the induced screening charge ϱ_s:

$$\boldsymbol{E}(\boldsymbol{G}+\boldsymbol{q},\omega) = -i(\boldsymbol{G}+\boldsymbol{q})V(\boldsymbol{G}+\boldsymbol{q},\omega). \qquad (10)$$

In linear response theory the dielectric tensor $\overleftrightarrow{\boldsymbol{\epsilon}}$ is defined by

$$D(G+q,\omega)=\sum_{G'q'}\vec{\vec{\epsilon}}_{GG'}(q,q',\omega)E(G'+q',\omega). \quad (11)$$

By our definitions D and E are longitudinal, i.e., parallel to q. Therefore, the DF refers to the longitudinal-longitudinal one.

Insertion of Eqs. (9) and (10), and some reordering of terms leads to the following equation:

$$4\pi\frac{G+q}{|G+q|^2}\varrho_s(G+q,\omega)=\sum_{G'q'}V(G'+q',\omega)[\delta_{GG'}\delta_{qq'}\vec{\vec{1}}$$
$$-\vec{\vec{\epsilon}}_{GG'}(q,q',\omega)](G'+q').$$

By taking the functional derivative with respect to the potential V, we introduce the polarization[17]

$$P_{GG'}(q,q',\omega)=\frac{\delta\varrho_s(G+q,\omega)}{\delta V(G'+q',\omega)}. \quad (12)$$

Then the equation can be solved for the dielectric tensor, yielding

$$\vec{\vec{\epsilon}}_{GG'}(q,q',\omega)=\delta_{GG'}\delta_{qq'}\vec{\vec{1}}$$
$$-4\pi\frac{(G+q)\otimes(G'+q')}{|G+q|^2|G'+q'|^2}P_{GG'}(q,q',\omega). \quad (13)$$

To get $\vec{\vec{\epsilon}}$ in an arbitrary basis it is advantageous to transform Eq. (13) into real space by the usual formula

$$\vec{\vec{\epsilon}}(r,r',\omega)=\frac{1}{\Omega}\sum_{qq'}\sum_{GG'}e^{i(G+q)\cdot r}\vec{\vec{\epsilon}}_{GG'}(q,q',\omega)e^{-i(G'+q')\cdot r'}. \quad (14)$$

$\Omega=N\Omega_{UC}$ denotes the crystal volume and Ω_{UC} the volume of the unit cell. With the help of

$$\sum_G\frac{G+q}{|G+q|^2}e^{i(G+q)\cdot(r-r_1)}=\frac{\Omega_{UC}}{4\pi i}\sum_R e^{iq\cdot R}\nabla_r\frac{1}{|r-r_1-R|} \quad (15)$$

we get

$$\vec{\vec{\epsilon}}(r,r',\omega)=\delta(r-r')\vec{\vec{1}}-\frac{1}{4\pi}\int d^3r_1\int d^3r_2 P(r_1,r_2,\omega)$$
$$\times\nabla_r\frac{1}{|r-r_1|}\otimes\nabla_{r'}\frac{1}{|r'-r_2|}. \quad (16)$$

Because this expression follows from pure classical considerations it is independent of the microscopic theory for the polarization. Taking the matrix elements between basis functions φ_{iq} yields the desired result

$$\vec{\vec{\epsilon}}_{ij}(q,\omega)=S_{ij}(q)\vec{\vec{1}}-\frac{1}{4\pi}\int d^3r_1\int d^3r_2 P(r_1,r_2,\omega)\Phi_{iq}^*(r_1)$$
$$\otimes\Phi_{jq}(r_2) \quad (17)$$

with the "orbital field" Φ defined by

$$\Phi_{iq}(r)=-\nabla\int d^3r'\frac{\varphi_{iq}(r')}{|r'-r|}. \quad (18)$$

We have used the diagonality of $\vec{\vec{\epsilon}}$ in q and q', which holds for any periodic lattice. The evaluation of the orbital field for a localized-basis set is done by a transformation to summations over the reciprocal and direct lattice. These calculations are described in the Appendix.

To be concrete, we specialize on the random phase approximation to the (time-ordered) polarization[17]

$$P_t(r,r',t,t')=-iG(r,r',t,t')G(r',r,t',t). \quad (19)$$

G is the one-particle Greens function, which is approximated by the resolvent of the LDA Hamiltonian. By introducing the eigenfunctions ψ_{nk} and eigenvalues E_{nk} of the Hamiltonian and switching to the retarded polarization one arrives at

$$P(r,r',\omega)=\sum_{nk}\sum_{n'k'}\psi_{nk}(r)\psi_{nk}^*(r')\psi_{n'k'}(r')\psi_{n'k'}^*(r)$$
$$\times\frac{f_{nk}-f_{n'k'}}{E_{nk}-E_{n'k'}-\omega-i\eta}. \quad (20)$$

f_{nk} denotes the Fermi distribution function and η a small positive value. With the definition of the M matrices

$$M_{n'n}^{iq}(k',k)=\int d^3r\,\psi_{n'k'}^*(r)\psi_{nk}(r)\Phi_{iq}^*(r), \quad (21)$$

we get

$$\vec{\vec{\epsilon}}_{ij}(q,\omega)=S_{ij}(q)\vec{\vec{1}}-\frac{1}{4\pi}\sum_{nk}\sum_{n'k'}$$
$$\times\frac{(f_{nk}-f_{n'k'})M_{n'n}^{iq}(k',k)\otimes[M_{n'n}^{jq}(k',k)]^*}{E_{nk}-E_{n'k'}-\omega-i\eta}. \quad (22)$$

Now the question arises, which basis functions should be used for the expansion of the dielectric function. Following the arguments given by Aryasetiawan and Gunnarson,[3,18] the Hilbert space spanned by ϵ^{-1} is given by all products of two wave functions, i.e., the set $\{\psi_{nk}\psi_{n'k'}\}$. If the wave functions are expanded in plane waves, the product basis consists again of ordinary plane waves and the last equation leads to the well-known Adler-Wiser formula.[19,20] Almost all calculations are along this line, which is appropriate for systems with three-dimensional periodicity. To our knowledge, there are only two approaches which expand the DF into other basis functions than plane waves. About 30 years ago Hanke and Sham[21] used tight-binding functions to calculate the macroscopic DF of diamond. In 1994 Aryasetiawan and Gunnarson[3] expanded ϵ^{-1} in a LMTO basis. The computational work was reduced by the atomic-sphere approximation (ASA) and by omitting roughly 3/4 of the product basis functions. Still, they found 70 to 100 functions per atom to be necessary.

In our calculations, we expand the wave functions in a linear combination of atomiclike orbitals. Thus, the method of Hanke and Sham should be well suited. But in their work the number of product functions is given by $N_{nn} \times N_{ao}^2$ with N_{nn} being the number of nearest neighbors entering the Bloch sums and N_{ao} being the number of atomic orbitals. The resulting number is acceptable only in the tight-binding limit, but explodes for an *ab initio* LCAO program. The method of Aryasetiawan and Gunnarson needs much less but still a large number of functions per atom and relies on the atomic-sphere approximation. The generalization to overlapping orbitals seems to be difficult.

In order to keep the number of functions low, we do not expand the DF into products of basis functions but an ordinary LCAO basis. Of course, this is worse than the proper product basis if the basis set is incomplete. But it might be a good approximation and converge to the true result with increasing number of functions. To investigate this behavior we calculate the microscopic DF $\epsilon_{\text{micro}}(\boldsymbol{q},\omega)$ as well as the macroscopic DF $\epsilon_{\text{macro}}(\omega)$ with the usual Adler-Wiser formula and our LCAO approach for different sets of localized functions.

Because $\epsilon_{\text{micro}}(\boldsymbol{q},\omega)$ and $\epsilon_{\text{macro}}(\omega)$ require the DF in Fourier representation (denoted by subscript F, we use double underscore for matrices)

$$\epsilon_{\text{micro}}(\boldsymbol{q},\omega) = [\underline{\underline{\epsilon}}_F(\boldsymbol{q},\omega)]_{\boldsymbol{G}=\boldsymbol{G}'=0}, \qquad (23)$$

$$\epsilon_{\text{macro}}(\omega) = \lim_{\boldsymbol{q}\to 0} \frac{1}{[\underline{\underline{\epsilon}}_F^{-1}(\boldsymbol{q},\omega)]_{\boldsymbol{G}=\boldsymbol{G}'=0}}, \qquad (24)$$

the scalar LCAO-DF $\underline{\epsilon} = \hat{\boldsymbol{q}} \cdot \underline{\underline{\tilde{\epsilon}}} \cdot \hat{\boldsymbol{q}}$ is transformed to Fourier space

$$\underline{\underline{\epsilon}}_F(\boldsymbol{q},\omega) = \underline{\underline{S}}^{FL}(\boldsymbol{q}) \underline{\underline{S}}^{-1}(\boldsymbol{q}) \underline{\epsilon}(\boldsymbol{q},\omega) \underline{\underline{S}}^{-1}(\boldsymbol{q}) [\underline{\underline{S}}^{FL}(\boldsymbol{q})]^+ \qquad (25)$$

$$\underline{\underline{\epsilon}}_F^{-1}(\boldsymbol{q},\omega) = \underline{\underline{S}}^{FL}(\boldsymbol{q}) [\underline{\epsilon}(\boldsymbol{q},\omega)]^{-1} [\underline{\underline{S}}^{FL}(\boldsymbol{q})]^+. \qquad (26)$$

The $\underline{S}$ matrices present in Eq. (25) cancel out in Eq. (26). The overlap integral $S_{Gi}^{FL}(\boldsymbol{q})$ between plane wave $(1/\sqrt{\Omega})e^{i(\boldsymbol{G}+\boldsymbol{q})\cdot\boldsymbol{r}}$ and basis function $\varphi_{i\boldsymbol{q}}(\boldsymbol{r})$ reduces to a one-dimensional integral, which is done numerically. Of course, only the head elements ($\boldsymbol{G}=\boldsymbol{G}'=0$) of $\underline{\underline{\epsilon}}_F$ and $\underline{\underline{\epsilon}}_F^{-1}$ need to be calculated.

By deriving the last two equations, the decomposition of unity, which reads in LCAO representation

$$\hat{I} = \sum_{ij\boldsymbol{k}} |i\boldsymbol{k}\rangle S_{ij}^{-1}(\boldsymbol{k}) \langle j\boldsymbol{k}| \qquad (27)$$

[with $\langle \boldsymbol{r}|i\boldsymbol{k}\rangle = \varphi_{i\boldsymbol{k}}(\boldsymbol{r})$ being LCAO functions], was used twice. Because of the incompleteness of the LCAO basis $\epsilon_{\text{micro}}(\boldsymbol{q},\omega)$ and $\epsilon_{\text{macro}}(\omega)$ are too small. This is corrected by a factor

$$F(\boldsymbol{q}) = [\underline{\underline{S}}^{FL}(\boldsymbol{q}) \underline{\underline{S}}^{-1}(\boldsymbol{q}) [\underline{\underline{S}}^{FL}(\boldsymbol{q})]^+]_{\boldsymbol{G}=\boldsymbol{G}'=0}^{-2}, \qquad (28)$$

which should be one, ideally, and is some measure of the unitarity of the transformation from LCAO to Fourier representation.

In the following we show results for the semiconductors diamond and GaAs. The integrals appearing in Eq. (21) as well as the matrix elements $\langle \psi_{n\boldsymbol{k}}|\exp[i(\boldsymbol{G}+\boldsymbol{q})\cdot\boldsymbol{r}]|\psi_{n'\boldsymbol{k}'}\rangle$ for the plane-wave DF are done by tabulating the wavefunctions and the orbital field (or the plane wave) in the unit cell and using the numerical integration scheme introduced in the preceding section. Therefore, the computational costs of both approaches are the same. Because the orbital field does not depend on the $\boldsymbol{k}$ vector its calculation does not enhance the numerical effort noticeable.

IV. APPLICATION TO DIAMOND

Diamond has the electronic configuration $1s^2 2s^2 2p^2$. Because of the covalent binding through sp^3 hybrid orbitals one expects local-field effects in the DF. The lattice constant was chosen to be 6.75 a_{Bohr}.

The electronic-structure calculations were performed with two special $\boldsymbol{k}$ points for sampling the irreducible wedge of the Brillouin zone and 26 614 integration points in the unit cell. Such a large number is necessary for a precise calculation of the factor $F(\boldsymbol{q})$. The eigenvalues of the Kohn-Sham Hamiltonian are already converged with 7975 integration points (less than 0.04 eV deviation in the valence bands). The band structure compares well with other results.[22–24] As usual in DFT-LDA calculations for semiconductors, the fundamental band gap is underestimated. We find a minimal band gap of 3.98 eV while the experiment gives 5.48 eV. At point Γ the calculated band gap is 5.49 eV and the experimental one is 7.3 eV (some measured energies are collected in Ref. 23). This shows that the underestimation of the conduction bands in LDA depends on the $\boldsymbol{k}$ point, so, a rigid scissor-operator shift is not a good approximation for this wide-gap semiconductor.

Dielectric function of diamond. We have calculated the DF in LCAO representation and transformed to Fourier space according to Eq. (25) and Eq. (26) for a small wave vector $\boldsymbol{q}=(0.0001,0,0)(2\pi/a)$. The correction factor $F(\boldsymbol{q})$ is shown in Fig. 1 against the number of LCAO basis functions. Remember that the parameter r_0 (Sec. II) is not optimized (e.g., by minimizing the total energy as in Refs. 22 and 25). Therefore, small basis sets such as single-ζ (minimal basis) and even polarized double-ζ ($1s\,2sp\,3spd$) do not give satisfactory bandstructures and large values for the factor $F(\boldsymbol{q})$. Even triple-ζ and further polarization up to $1s\,2sp\,3spd\,4spdf$ yield $\approx 3\%$ deviation from 1. With the help of off-site functions much smaller values are reached with a comparable number of basis functions. 46 functions per atom, divided into atomic orbitals $1s\,2sp\,3spd\,4spdf$ and off-site functions $4spdf$, yield a correction factor of $F(\boldsymbol{q})=1.0012$.

In Fig. 2 the DF of diamond evaluated according to the Adler-Wiser formula is shown. We have calculated the dielectric matrix $\epsilon_{GG'}(\boldsymbol{q},\omega)$ in Fourier space for 65 reciprocal lattice vectors $\boldsymbol{G}$, $\boldsymbol{G}'$. Test calculations with a higher number of $\boldsymbol{G}$ vectors show that this number of $\boldsymbol{G}$ vectors is sufficient for describ-
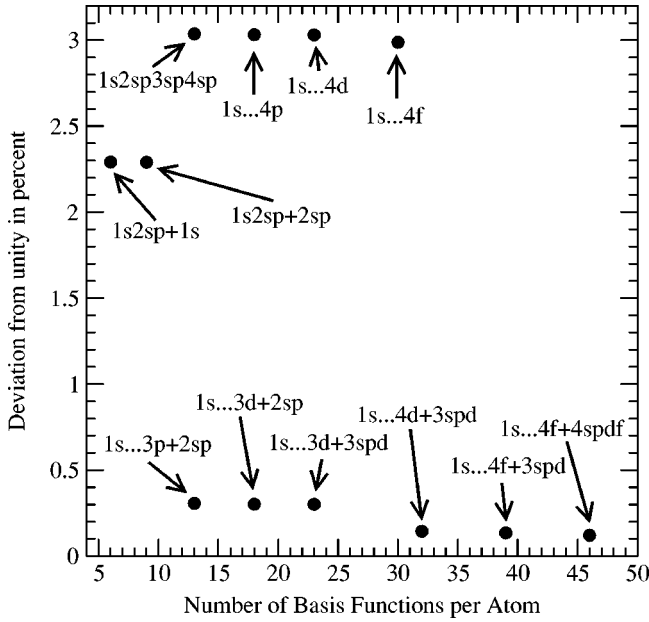
FIG. 1. The figure displays the quality of the transformation from LCAO space to Fourier space for different LCAO sets for diamond. The ordinate shows $(F-1)\times 100\%$, whereas F is unity for a complete basis set. The labels indicate the constituting orbitals. For example $1s\cdots 3d+3spd$ means that 14 spinless orbitals ($1s\cdots 3d=1s$, $2sp$, and $3spd$) are located at diamond atoms and nine functions of s, p, and d type are placed in the interstitial (denoted by $+3spd$). The wave vector is $q=(0.0001,0,0)(2\pi/a)$.

ing local-field effects (LFE's). The solid curve shows the macroscopic DF (i.e., with LFE) according to Eq. (24). The dashed curve shows the microscopic DF (i.e., without LFE) according to Eq. (23). The wave vector is $q=(0.0001,0,0)$
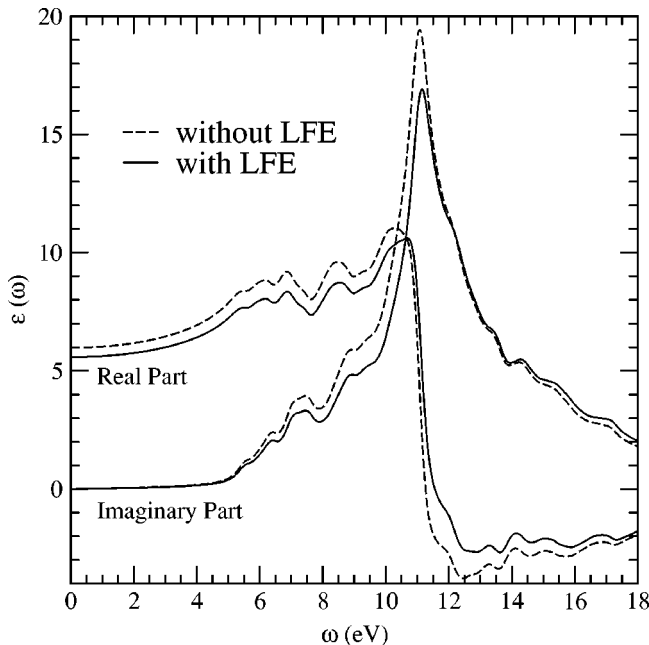

FIG. 2. Dielectric function of diamond for $q=(0.0001,0,0)$ $\times(2\pi/a)$. Full (broken) curve denotes macroscopic (microscopic) DF calculated in plane-wave representation.
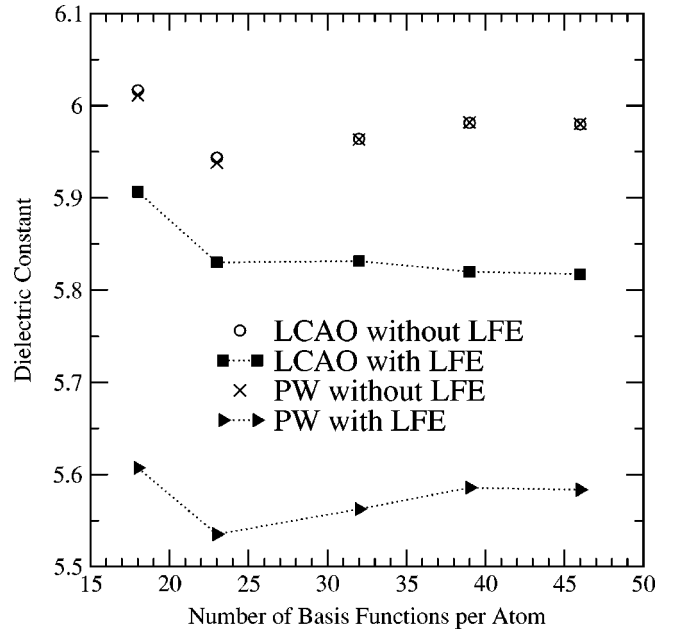

FIG. 3. Dielectric constant of diamond for $q=(0.0001,0,0)$ $\times(2\pi/a)$ against the number of LCAO functions.

$\times(2\pi/a)$ and the broadening parameter amounts to $\eta=0.27$ eV. The Brillouin zone was sampled with 1154 k vectors. Wave functions are expanded into 92 LCAO functions and tabulated at 26 614 real-space integration points.

The inclusion of LFE has no great influence on the DF for such a small wave vector. The main peak is slightly shifted to higher energies and in general the curve is somewhat damped. The effect increases with higher q as shown in Ref. 8. Experimentally, the main peak is located at 11.6 eV (Ref. 26) while we see it at 11.08 eV without LFE and at 11.15 eV with LFE. This good agreement is surprising at first sight, because the band gap in our calculations comes out to be 1.5 to 1.8 eV too small. As has been shown by recent investigations,[2] this is due to the cancellation of two many-body effects. First, the calculation of quasiparticle energies corrects the band gap and therefore shifts the DF to higher energies. If additionally excitonic effects are considered this shift is to some amount reversed. The same argument holds for the static dielectric constant $\epsilon_0=\epsilon_{\mathrm{macro}}(\omega=0)$. In our calculation we found $\epsilon_0=5.58$. This is 1.8% lower than the experimental value of $\epsilon_0=5.68$.[26] If the LDA band gap is corrected, either by a rigid scissor-operator shift of the conduction bands or by proper evaluation of the quasiparticle energies, the static dielectric constant is underestimated by 16%.[2]

Calculating the DF in LCAO representation, i.e., along the way outlined in Sec. III, leads to results very close to the previous. Especially if LFE are neglected the curves are indistinguishable. The evaluation of the macroscopic DF according to Eqs. (24) and (26) is more difficult. The convergence with increasing number of basis functions to the plane-wave result is slow, as can be seen in Fig. 3. Here we show the dielectric constant ϵ_0 for different LCAO sets. It should be noted that the difference between LCAO and plane-wave results concerns the expansion of the DF only. In both calcu-
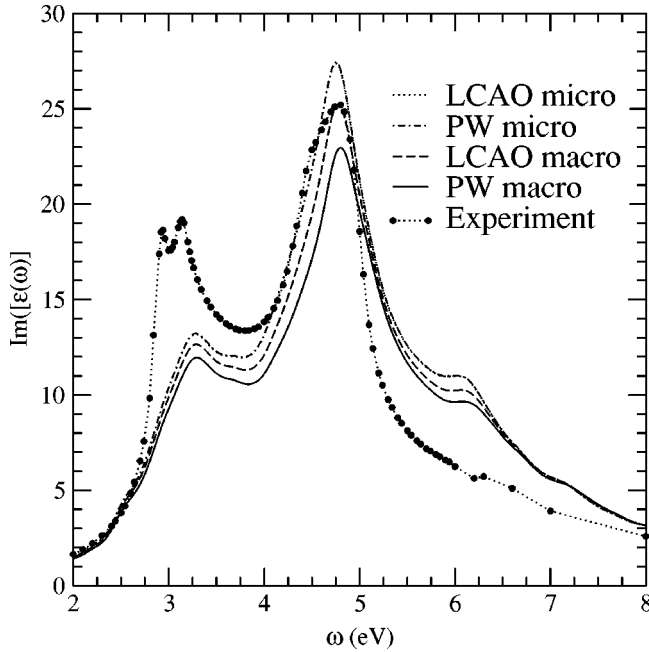
FIG. 4. Imaginary part of the DF of GaAs for $q = (0.0001,0,0) \times (2\pi/a)$.

lations wave functions are expanded in the same LCAO basis set. Without LFE, LCAO results (open circles) and plane-wave results (crosses) are the same. Inclusion of LFE leads to deviations between LCAO results (squares) and plane-wave values (triangles). Nevertheless, the difference decreases with increasing number of LCAO functions. We were not able to include more functions because a higher number of integration points is ruled out by limited computational capacity.

V. APPLICATION TO GaAs

GaAs is a covalently bound III-V semiconductor, which crystallizes in zincblende structure. As for diamond, off-site functions located in the interstitial greatly enhance the quality of the atomic-orbital basis. In order to eliminate effects from core orthogonalization, we performed all-electron calculations with the atomic orbitals $1s$ to $4f$ and off-site functions of s, p, and d character, yielding 39 functions per atom. The factor $F(q)$ defined in Sec. III has a value of 1.002 indicating a good quality of the basis set. The calculated band gap of 1.35 eV is too small by 0.17 eV compared with experiment[27] due to the local density approximation. Notice that the theoretical band gap in our LCAO calculation is larger than in pseudopotential plane-wave calculations, as was observed also by earlier LCAO calculation, see, for example, Ref. 28.

The DF is calculated with 6007 k points in the Brillouin zone and a broadening of $\eta = 0.16$ eV. Real-space integration is done with 7957 good lattice points in the unit cell. For a better comparison of the DF with experiment, we shifted the conduction bands by 0.6 eV to higher values. This shift does not restore the experimental band gap but the position of the main peak in $\text{Im}\epsilon_{\text{macro}}(\omega)$. In Fig. 4 the imaginary part

of the DF is shown. The curves labeled "PW macro" and "PW micro" are calculated with the Adler-Wiser formula, i.e., in plane-wave representation, with and without LFE, respectively. The dielectric matrix was evaluated for 65 reciprocal lattice vectors which are enough for describing LFE. The curves labeled "LCAO macro" and "LCAO micro" are calculated with the LCAO representation of ϵ with and without LFE. The microscopic DF calculated in LCAO and PW representation coincide, whereas the macroscopic LCAO-DF differs from the PW-DF. Obviously, the LCAO-DF lies in between the microscopic DF and the macroscopic PW-DF, which shows that not all LFE could be caught because of the too small basis set. Anyway, the deviations of all curves from experiment[29] show that there are other sources of error, which are much larger. As in the case of diamond, excitonic effects are responsible for the shift of spectral weight from higher energies to lower energies, which brings the theoretical curve very close to the measured DF.[30] The inclusion of LFE becomes important for higher energies than we considered. In the far UV regime, that means if excitations from semicore states set in, LFE show drastic influence on optical spectra.[31]

VI. CONCLUSIONS

We have introduced a formula which allows the evaluation of the dielectric tensor in an arbitrary basis. For the case of a LCAO basis, we developed an efficient scheme to calculate the matrix elements with the help of the Ewald summation technique. This approach opens the possibility to calculate the DF for systems which do not have the full periodicity and therefore cannot be described in Fourier representation.

To account for the incompleteness of the transformation from the LCAO set to a plane-wave basis, we defined a factor $F(q)$. With optimization of this factor the microscopic DF of diamond and GaAs are in very good agreement with plane-wave results, even for small basis sets. The macroscopic DF is not such well reproduced. This is not a serious drawback of the proposed method. Although much interest has been drawn on LFE in the past, comparison with experiment and more advanced calculations including excitonic effects, show that LFE do not improve the DF significantly in the low energy region for small wave vectors q.

APPENDIX: THE ORBITAL FIELD

In this section we describe the calculation of the orbital fields

$$\boldsymbol{\Phi}_{iq}(\boldsymbol{r}) = -\boldsymbol{\nabla} \int d^3 r' \frac{\varphi_{iq}(\boldsymbol{r}')}{|\boldsymbol{r}' - \boldsymbol{r}|} \tag{A1}$$

for LCAO basis functions given by Eq. (8). $u_{At,nlm}(\boldsymbol{r}) = Y_{lm}(\hat{\boldsymbol{r}}) R_{At,nl}(r)$ is a solution of the atomic Schrödinger equation composed of a radial function $R_{At,nl}(r)$ and a spherical harmonic $Y_{lm}(\hat{\boldsymbol{r}})$. The lumped index i denotes kind and position s_i of the atom and quantum numbers nlm. With the multipole expansion

$$\frac{1}{|\mathbf{r}'-\mathbf{r}|}=\sum_{l'm'}\frac{4\pi}{2l'+1}\frac{r_<^{l'}}{r_>^{l'+1}}Y_{l'm'}(\hat{\mathbf{r}})Y^*_{l'm'}(\hat{\mathbf{r}}'),\quad(\text{A2})$$

$$r_>=\max(r,r'),\quad r_<=\min(r,r')\qquad(\text{A3})$$

the angular part of the integral (A1) can be done. Because of the orthogonality of spherical harmonics the summation over the angular momenta $l'm'$ cancels. There remains a sum over lattice vectors $\mathbf{R}$

$$\mathbf{\Phi}_{iq}(\mathbf{r})=-\nabla\sum_{\mathbf{R}}e^{i\mathbf{q}\cdot\mathbf{R}}Y_{lm}(\hat{\mathbf{t}})\widetilde{R}_{At,nl}(t)\qquad(\text{A4})$$

with the abbreviation $\mathbf{t}=\mathbf{r}-\mathbf{R}-\mathbf{s}_i$ and the transformed radial functions

$$\widetilde{R}_{At,nl}(t)=\frac{4\pi}{2l+1}\left[t^{-l-1}\int_0^t r^{l+2}R_{At,nl}(r)dr\right.$$
$$\left.+t^l\int_t^\infty r^{1-l}R_{At,nl}(r)dr\right].\qquad(\text{A5})$$

Because of $\widetilde{R}_{At,nl}(t)\xrightarrow{t\to\infty}c_{At,nl}t^{-l-1}$, with a constant $c_{At,nl}$, the lattice sum can be decomposed into two parts

$$\mathbf{\Phi}_{iq}(\mathbf{r})=-\nabla\sum_{\mathbf{R}}e^{i\mathbf{q}\cdot\mathbf{R}}Y_{lm}(\hat{\mathbf{t}})\left[\widetilde{R}_{At,nl}(t)-\frac{c_{At,nl}}{t^{l+1}}\right]$$

$$-\nabla\sum_{\mathbf{R}}e^{i\mathbf{q}\cdot\mathbf{R}}Y_{lm}(\hat{\mathbf{t}})\frac{c_{At,nl}}{t^{l+1}}.\qquad(\text{A6})$$

The first sum converges already rapidly while the second one can be further analytically treated. We therefore introduce a differential operator $\hat{D}_{lm}$ with the property

$$Y_{lm}(\hat{\mathbf{t}})\frac{1}{t^{l+1}}=\hat{D}_{lm}\frac{1}{t}.\qquad(\text{A7})$$

We are using real-valued linear combinations of spherical harmonics. The first few Y_{lm} and the corresponding operators $\hat{D}_{lm}$ are given by

$$Y_s(\hat{\mathbf{r}})=\sqrt{\frac{1}{4\pi}}\quad\hat{D}_s=\sqrt{\frac{1}{4\pi}},$$

$$Y_{px}(\hat{\mathbf{r}})=\sqrt{\frac{3}{4\pi}}\frac{x}{r}\quad\hat{D}_{px}=-\sqrt{\frac{3}{4\pi}}\partial_x,$$

$$Y_{py}(\hat{\mathbf{r}})=\sqrt{\frac{3}{4\pi}}\frac{y}{r}\quad\hat{D}_{py}=-\sqrt{\frac{3}{4\pi}}\partial_y,$$

$$Y_{pz}(\hat{\mathbf{r}})=\sqrt{\frac{3}{4\pi}}\frac{z}{r}\quad\hat{D}_{pz}=-\sqrt{\frac{3}{4\pi}}\partial_z.$$

So, the spherical harmonic is replaced by $\hat{D}_{lm}$, which can be taken out of the sum. Then, one arrives essentially at the simple task to calculate

$$S(\mathbf{r})=\sum_{\mathbf{R}}e^{i\mathbf{q}\cdot\mathbf{R}}\frac{1}{|\mathbf{r}-\mathbf{R}|}.\qquad(\text{A8})$$

This can be done by the Ewald summation technique:[32]

$$S(\mathbf{r})=\frac{4\pi}{\Omega_{uc}}\sum_{\mathbf{G}}\frac{e^{i(\mathbf{G}+\mathbf{q})\cdot\mathbf{r}}}{|\mathbf{G}+\mathbf{q}|^2}e^{-|\mathbf{G}+\mathbf{q}|^2/4\alpha^2}$$

$$+\sum_{\mathbf{R}}e^{i\mathbf{q}\cdot\mathbf{R}}\frac{\text{erfc}(\alpha|\mathbf{r}-\mathbf{R}|)}{|\mathbf{r}-\mathbf{R}|}.\qquad(\text{A9})$$

$\text{erfc}(x)$ is the complementary error function, which goes fast to zero for $x\to\infty$. The real parameter α controls the convergence of the sums over reciprocal lattice vectors $\mathbf{G}$ and direct lattice vectors $\mathbf{R}$. They both converge exponentially. The final result for the orbital field is obtained by taking the derivatives implied by $\hat{D}_{lm}$ and ∇, which leads to somewhat unpleasant long formulas. The case $\mathbf{t}\to\mathbf{0}$ has to be treated carefully, for example, by Taylor expansion. As can be seen in the last equation, the orbital field cannot be calculated for $\mathbf{q}=\mathbf{0}$. But owing to the Ewald technique, $\mathbf{q}$ can be very small without affecting the convergence properties. We have programmed the resulting equations for l up to 3. The summation turns out to be numerically stable and very fast.

---

[1] L.X. Benedict, E.L. Shirley, and R.B. Bohn, Phys. Rev. Lett. **80**, 4514 (1998).

[2] B. Arnaud and M. Alouani, Phys. Rev. B **63**, 085208 (2001).

[3] F. Aryasetiawan and O. Gunnarsson, Phys. Rev. B **49**, 16 214 (1994).

[4] M.-Z. Huang and W.Y. Ching, Phys. Rev. B **47**, 9449 (1992).

[5] M. Yu, S.E. Ulloa, and D.A. Drabold, Phys. Rev. B **61**, 2626 (2000).

[6] F. Kootstra, P.L. de Boeij, and J.G. Snijders, Phys. Rev. B **62**, 7071 (2000).

[7] V.I. Gavrilenko and F. Bechstedt, Phys. Rev. B **55**, 4343 (1996).

[8] S. Waidmann, M. Knupfer, B. Arnold, J. Fink, A. Fleszar, and W. Hanke, Phys. Rev. B **61**, 10 149 (1999).

[9] D.E. Ellis, Int. J. Quantum Chem. **IIs**, 35 (1968).

[10] I.H. Sloan and P.J. Kachoyan, SIAM (Soc. Ind. Appl. Math.) J. Numer. Anal. **24**, 116 (1987).

[11] G. te Velde and E.J. Baerends, Phys. Rev. B **44**, 7888 (1991).

[12] H. Eschrig, *Optimized LCAO Method* (Springer Verlag, Berlin, 1989).

[13] D.G. Anderson, J. Comput. Math. **12**, 547 (1964).

[14] V. Eyert, J. Comput. Phys. **124**, 271 (1996).

[15] D.M. Ceperley and B.J. Alder, Phys. Rev. Lett. **45**, 566 (1980).

[16] J.P. Perdew and A. Zunger, Phys. Rev. B **23**, 5048 (1981).

[17] L. Hedin and S. Lundqvist, in *Solid State Physcis 23*, edited by H. Ehrenreich, F. Seitz, and D. Turnbull (Academic, New York, 1969).

[18] T. Miyake and F. Aryasetiawan, Phys. Rev. B **61**, 7172 (2000).

[19] S.L. Adler, Phys. Rev. **126**, 413 (1962).

[20] N. Wiser, Phys. Rev. **129**, 62 (1963).

[21] W. Hanke and L.J. Sham, Phys. Rev. B **12**, 4501 (1975).

[22] K. Koepernik and H. Eschrig, Phys. Rev. B **59**, 1743 (1998).

[23] B. Arnaud and M. Alouani, Phys. Rev. B **62**, 4464 (2000).

[24] X. Chen, J.-M. Langlois and W.A. Goddard III, Phys. Rev. B **52**, 2348 (1995).

[25] J. Junquera, O. Paz, D. Sanchez-Portal, and E. Artacho, Phys. Rev. B **64**, 235111 (2001).

[26] *CRC Handbook of Chemistry and Physics*, 77th Edition, edited by D.R. Linde and H.P.R. Frederikse (CRC Press, Florida, 1996), pp. 12–133.

[27] R. Hott, Phys. Rev. B **44**, 1057 (1991).

[28] Z.Q. Gu and W.Y. Ching, Phys. Rev. B **49**, 10 958 (1994).

[29] E.D. Palik, *Handbook of Optical Constants of Solids* (Academic, New York, 1985).

[30] M. Rohlfing and S.G. Louie, Phys. Rev. Lett. **81**, 2312 (1998).

[31] E.E. Krasovskii and W. Schattke, Phys. Rev. B **63**, 235112 (2001).

[32] P.P. Ewald, Ann. Phys. (N.Y.) **64**, 253 (1921).